

# A DC/DC Buck-Boost Converter–Inverter–DC Motor System: Sensorless Passivity-Based Control

Eduardo Hernández-Márquez<sup>1,2</sup>, Ramón Silva-Ortigoza<sup>1</sup>, José Rafael García-Sánchez<sup>1</sup>,  
Mariana Marcelino-Aranda<sup>3</sup>, and Griselda Saldaña-González<sup>4</sup>

<sup>1</sup>Área de Mecatrónica, CIDETEC, Instituto Politécnico Nacional, Mexico City 07700, Mexico

<sup>2</sup>Departamento de Mecatrónica, Instituto Tecnológico Superior de Poza Rica, Poza Rica, Ver. 93230, Mexico

<sup>3</sup>SEPI, UPIICSA, Instituto Politécnico Nacional, Mexico City 08400, Mexico

<sup>4</sup>División de Mecatrónica, Universidad Tecnológica de Puebla, Puebla, Pue. 72300, Mexico

Corresponding author: R. Silva-Ortigoza (rsilvao@ipn.mx)

This work was supported by Secretaría de Investigación y Posgrado del Instituto Politécnico Nacional, México.

The work of E. Hernández-Márquez and J. R. García-Sánchez has been supported by CONACYT-México and BEIFI scholarships.

Likewise, R. Silva-Ortigoza and M. Marcelino-Aranda acknowledge financial support from SNI-México and IPN programs EDI and COFFA. Finally, G. Saldaña-González thanks financial support from the Universidad Tecnológica de Puebla.

**Abstract**—This paper presents a passivity-based control for the DC/DC Buck-Boost converter–inverter–DC motor system. Such control exploits the energy structure associated with the system error dynamics. This in order to solve the trajectory tracking task for both the converter voltage and motor bidirectional angular velocity, without using electromechanical sensors. The successful experimental validation of the proposed control is performed in a built prototype of the system, using Matlab-Simulink and a DS1104 board.

**Index Terms**—DC/DC Buck-Boost converter, inverter, DC motor, passivity-based control, trajectory tracking.

## I. INTRODUCTION

Applications that have been profited from using electronic power converters can be found in mechanisms [1], robotics [2], [3], electric cars [4], and airplanes [5], among others. In such applications, in general, their correct operation involves high precision movements. These movements are accomplished through the connection of power electronics converters and motors both commanded with control strategies.

In recent years, a great interest has arisen in the design of controls for regulation and trajectory tracking tasks in a DC/DC converter–DC motor system. In that direction, works where the aforementioned tasks were solved, for several topologies of DC/DC converters connected to DC motors, are [6]–[22]. The contribution of these works summarizes in driving the motor shaft in only one direction. This limitation comes from the operating principle of DC/DC converters because they only can supply unipolar voltage. Thus, in order to face such a problem, research related to bipolar voltage supply for DC motors using DC/DC converters has been presented in [23]–[29]. In those works, an *inverter* circuit is connected between the converter and motor, allowing the bidirectional driving of both position and angular velocity of the motor shaft. Thus, Ortigoza *et al.* presented the experimental validation of a mathematical model for the Buck converter–inverter–DC motor system and the design

of a passive tracking control in [23] and [24], respectively. Also, García-Rodríguez *et al.* developed a mathematical model for the Boost converter–inverter–DC motor system in [25]. Whereas Márquez *et al.* proposed a model for the DC/DC Buck-Boost converter–inverter–DC motor system, validated through simulation for constant duty cycles in [26] and experiments for time-varying duty cycles in [27]. Likewise, Hernández-Márquez *et al.* designed a passive control for the regulation of such a system in [28]. Lastly, Linares-Flores *et al.* in [29], via a passive control, solved the regulation task associated with the Sepic converter–inverter–DC motor system.

According to the presented review, it was found that the angular velocity control has been solved unidirectionally [20], [21] and bidirectionally [28] for the configurations that use the Buck-Boost converter. Therefore, as a continuation of [28], a control for the bidirectional trajectory tracking associated with the DC/DC Buck-Boost converter–inverter–DC motor system is presented here. The control design is based on passivity and its stability analysis is verified via Lyapunov and the Sylvester criterion [30]. Also, the control is experimentally tested using Matlab-Simulink and a DS1104 board in a built prototype of the system.

The structure of the work is as follows. Section II describes and develops the mathematical model of the system under study. Whereas the control design is presented in Section III. The reference variables are shown in Section IV. Section V reports the built prototype and the results obtained from the experiments. Lastly, conclusions and future work are given in Section VI.

## II. DC/DC BUCK-BOOST CONVERTER–INVERTER–DC MOTOR SYSTEM

This section describes the parts composing the DC/DC Buck-Boost converter–inverter–DC motor system. Later, the associated average model is presented.

### A. System description

The electronic diagram of the system under study is shown in Fig. 1, which is composed of the following stages:

- *DC/DC Buck-Boost converter.* This reduces or increases the voltage at the input of the inverter. The converter comprises a power supply  $E$ , a transistor  $Q_1$  that regulates the voltage  $v$  at the terminals of the capacitor  $C$  and the load  $R$ , an inductance  $L$  through which the current  $i$  flows, and a diode  $D$ .
- *Inverter.* This stage of the system aims to change the direction of the current flow entering the motor. The inverter is composed of four transistors, two denoted by  $Q_2$  and the others by  $\bar{Q}_2$ . If  $Q_2$  is activated, then  $\bar{Q}_2$  is deactivated and vice versa.
- *DC motor.* The parameters  $R_a$  and  $L_a$  represent the resistance and inductance of the motor armature, respectively. Meanwhile,  $i_a$  and  $\omega$  correspond to the armature current and angular velocity. Implicitly, the parameters  $J$ ,  $b$ ,  $k_e$ , and  $k_m$  are considered in the motor and represent the moment of inertia of the rotor plus the inertia of the load, the coefficient of viscous friction, the constants of counter electromotive force and torque.

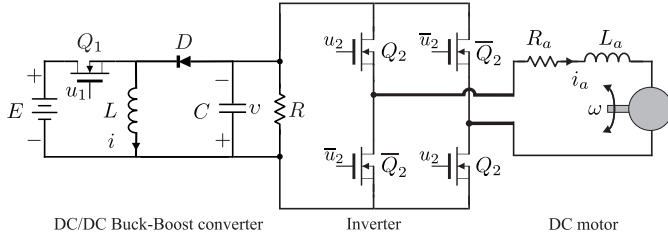


Figure 1. DC/DC Buck-Boost converter-inverter-DC motor system.

### B. Average model

According to [26] and [27] the average model of the DC/DC Buck-Boost converter-inverter-DC motor system, deduced by using the Kirchhoff laws and the mathematical model of the DC motor, is given by,

$$\begin{aligned} L \frac{di}{dt} &= Eu_{1av} + (1 - u_{1av})v, \\ C \frac{dv}{dt} &= -(1 - u_{1av})i - \frac{v}{R} - i_a u_{2av}, \\ L_a \frac{di_a}{dt} &= vu_{2av} - R_a i_a - k_e \omega, \\ J \frac{d\omega}{dt} &= k_m i_a - b\omega, \end{aligned} \quad (1)$$

where  $u_{1av} \in [0, 1]$  and  $u_{2av} \in [-1, 1]$  are the average system inputs, which allow the appropriate driving of  $v$  and  $\omega$  via a control law. The rest of the variables and constants associated with the model (1) have been previously declared.

An alternative representation for (1) that is useful in the design of the control scheme, based on [31], is determined by,

$$\mathcal{A}\dot{x} = [\mathcal{J}(u_{av}) - \mathcal{R}]x + \mathcal{B}u_{av}, \quad (2)$$

with

$$\begin{aligned} \mathcal{A} &= \text{diag}[L, C, L_a, J], \quad \mathcal{R} = \text{diag}\left[0, \frac{1}{R}, R_a, b\right], \\ \mathcal{J}(u_{av}) &= \begin{bmatrix} 0 & -(u_{1av} - 1) & 0 & 0 \\ u_{1av} - 1 & 0 & -u_{2av} & 0 \\ 0 & u_{2av} & 0 & -k_e \\ 0 & 0 & k_m & 0 \end{bmatrix}, \\ \mathcal{B} &= \begin{bmatrix} E & 0 \\ 0 & 0 \\ 0 & 0 \\ 0 & 0 \end{bmatrix}, \quad x = \begin{bmatrix} i \\ v \\ i_a \\ \omega \end{bmatrix}, \quad u_{av} = \begin{bmatrix} u_{1av} \\ u_{2av} \end{bmatrix}. \end{aligned}$$

Note that  $\mathcal{A}^{n \times n}$  is a symmetric and positive definite matrix,  $\mathcal{R}^{n \times n}$  a symmetric and positive semidefinite matrix that represents the dissipative terms,  $\mathcal{J}(u_{av})^{n \times n}$  an antisymmetric matrix (due to  $k_e = k_m$  [32]) representing the conservative part of the system,  $\mathcal{B}^{n \times m}$  a constant matrix,  $x^{n \times 1}$  the state vector of the system, and  $u_{av}^{m \times 1}$  the average control vector of the system. In this paper  $n = 4$  and  $m = 2$ .

### III. DESIGN OF THE PASSIVE CONTROL

A tracking control for the DC/DC Buck-Boost converter-inverter-DC motor system is proposed in this section. Such a control uses the *exact tracking error dynamics passive output feedback* (ETEDPOF) of the system [31].

The desired dynamics associated with (2), for the reference variables  $x^*$   $y$   $u_{av}^*$ , is determined by,

$$\mathcal{A}\dot{x}^* = [\mathcal{J}(u_{av}^*) - \mathcal{R}]x^* + \mathcal{B}u_{av}^*. \quad (3)$$

By subtracting (3) from (2) it is obtained:

$$\begin{aligned} \mathcal{A}(\dot{x} - \dot{x}^*) &= [\mathcal{J}(u_{av}) - \mathcal{R}](x - x^*) + [\mathcal{J}(u_{av}) - \mathcal{J}(u_{av}^*)]x^* \\ &\quad + \mathcal{B}(u_{av} - u_{av}^*). \end{aligned} \quad (4)$$

Since  $\mathcal{J}(u_{av})$  and  $\mathcal{J}(u_{av}^*)$  can be expressed, for  $m$  inputs, as:

$$\begin{aligned} \mathcal{J}(u_{av}) &= \mathcal{J}_0 + \sum_{i=1}^m \mathcal{J}_i u_{iav}, \\ \mathcal{J}(u_{av}^*) &= \mathcal{J}_0 + \sum_{i=1}^m \mathcal{J}_i u_{iav}^*, \end{aligned} \quad (5)$$

where  $\mathcal{J}_0$  is a constant antisymmetric matrix independent of the inputs  $u_{iav}$  and  $u_{iav}^*$ , whereas  $\mathcal{J}_i$  are antisymmetric constant matrices associated with the inputs. Then,

$$\mathcal{J}(u_{av}) - \mathcal{J}(u_{av}^*) = \sum_{i=1}^m \mathcal{J}_i (u_{iav} - u_{iav}^*). \quad (6)$$

After replacing (6) in (4) the following is obtained:

$$\begin{aligned} \mathcal{A}(\dot{x} - \dot{x}^*) &= [\mathcal{J}(u_{av}) - \mathcal{R}](x - x^*) \\ &\quad + \underbrace{[\mathcal{B} + (\mathcal{J}_1 x^*, \dots, \mathcal{J}_m x^*)]}_{=: \mathcal{B}^*} (u_{av} - u_{av}^*). \end{aligned} \quad (7)$$

Now, let the state and the control errors be defined as:

$$e = x - x^*, \quad e_{u_{av}} = u_{av} - u_{av}^*. \quad (8)$$

By considering (7) and (8) the error dynamics in open-loop is given by,

$$\mathcal{A}\dot{e} = [\mathcal{J}(u_{av}) - \mathcal{R}]e + \mathcal{B}^*e_{u_{av}}. \quad (9)$$

Thus, according to the ETEDPOF, the control  $e_{u_{av}}$  that achieves  $e \rightarrow 0$  is determined by,

$$e_{u_{av}} = -\Gamma\mathcal{B}^{*T}e, \quad (10)$$

with  $\Gamma = \text{diag}[\gamma_1, \gamma_2, \dots, \gamma_m] > 0$ . In order to show that  $e \rightarrow 0$ , (10) is replaced in (9) and the following error dynamics in closed-loop is obtained:

$$\mathcal{A}\dot{e} = [\mathcal{J}(u_{av}) - \mathcal{R}]e - \mathcal{B}^*\Gamma\mathcal{B}^{*T}e, \quad (11)$$

whose stability analysis is performed via the Lyapunov function candidate

$$V(e) = \frac{1}{2}e^T\mathcal{A}e. \quad (12)$$

The time-derivative of (12) along (11) is given by

$$\dot{V}(e) = e^T\mathcal{A}\dot{e} = -e^T[\mathcal{R} + \mathcal{B}^*\Gamma\mathcal{B}^{*T}]e,$$

which guaranties that  $e \rightarrow 0$  as long as

$$\mathcal{R} + \mathcal{B}^*\Gamma\mathcal{B}^{*T} > 0. \quad (13)$$

The latter is easily verified by invoking Sylvester criterion [30], since all principal diagonal minors of matrix  $[\mathcal{R} + \mathcal{B}^*\Gamma\mathcal{B}^{*T}]$ , associated with system (2) in closed-loop with (10), are positive. Thus, the control based on the ETEDPOF, for the DC/DC Buck-Boost converter–inverter–DC motor system, is given by

$$e_{u_{av}} = -\Gamma\mathcal{B}^{*T}e, \quad (14)$$

with:

$$e_{u_{av}} = \begin{bmatrix} e_{u_{1av}} \\ e_{u_{2av}} \end{bmatrix} = \begin{bmatrix} u_{1av} - u_{1av}^* \\ u_{2av} - u_{2av}^* \end{bmatrix}, \quad \Gamma = \begin{bmatrix} \gamma_1 & 0 \\ 0 & \gamma_2 \end{bmatrix} > 0,$$

$$\mathcal{B}^* = \begin{bmatrix} E - v^* & 0 \\ \alpha & -\frac{b\omega^*}{k_m} \\ 0 & v^* \\ 0 & 0 \end{bmatrix}, \quad e = \begin{bmatrix} e_1 \\ e_2 \\ e_3 \\ e_4 \end{bmatrix} = \begin{bmatrix} i - i^* \\ v - v^* \\ i_a - i_a^* \\ \omega - \omega^* \end{bmatrix},$$

where

$$\alpha = \left( \frac{v^* - E}{E} \right) \left[ \left( \frac{R_a b}{k_m} + k_m \right) \left( \frac{b\omega^{*2}}{k_m v^*} \right) + \frac{v^*}{R} \right],$$

and  $i^*, v^*, i_a^*, \omega^*, u_{1av}^*, u_{2av}^*$  are the reference variables of the system. Thus, (14) can be written explicitly as:

$$\begin{bmatrix} u_{1av} \\ u_{2av} \end{bmatrix} = \begin{bmatrix} u_{1av}^* - \gamma_1(v^* - E)(-e_1 + \frac{\alpha}{E}e_2) \\ u_{2av}^* - \gamma_2\left(-\frac{b\omega^*}{k_m}e_2 + v^*e_3\right) \end{bmatrix}. \quad (15)$$

#### IV. REFERENCE VARIABLES

The implementation of control (15) requires the dynamics of the reference variables  $i^*, v^*, i_a^*, \omega^*, u_{1av}^*$ , and  $u_{2av}^*$ , which are associated with (1). In that direction, according to [27], a possible representation in terms of  $v$  and  $\omega$  is determined by,

$$i = \frac{v - E}{E} \left[ \frac{v}{R} + \left( \frac{J\dot{\omega} + b\omega}{k_m v} \right) \times \left( \frac{L_a J}{k_m} \ddot{\omega} + \frac{L_a b + R_a J}{k_m} \dot{\omega} + \left( \frac{R_a b}{k_m} + k_m \right) \omega \right) \right], \quad (16)$$

$$i_a = \frac{1}{k_m} (J\dot{\omega} + b\omega), \quad (17)$$

$$u_{1av} = \frac{1}{E - v} \left( L \frac{di}{dt} - v \right), \quad (18)$$

$$u_{2av} = \left( \frac{L_a J}{k_m} \right) \frac{\ddot{\omega}}{v} + \left( \frac{L_a b + R_a J}{k_m} \right) \frac{\dot{\omega}}{v} + \left( \frac{R_a b}{k_m} + k_m \right) \frac{\omega}{v}. \quad (19)$$

In this way, the reference variables  $i^*, i_a^*, u_{1av}^*$ , and  $u_{2av}^*$  are obtained when  $v^*$  and  $\omega^*$  are replaced in (16)–(19).

#### V. BUILT PROTOTYPE AND EXPERIMENTAL RESULTS

In this section, the prototype built of the system under study is described. Subsequently, the experimental results of such a prototype in closed-loop are presented. Lastly, comments on the obtained results are given.

##### A. Built prototype

The electronic diagram of the built prototype, and its connections to the control by ETEDPOF (15) and the DS1104 board, is shown in Fig. 2. The blocks composing the experimental platform presented in Fig. 2 are described below. *DC/DC Buck-Boost converter–inverter–DC motor system*. This block corresponds to the system under study. The parameters of the Buck-Boost converter were selected as follows:

$$R = 64 \, \Omega, \quad C = 114.4 \, \mu\text{F}, \quad L = 4.94 \, \text{mH}, \quad E = 24 \, \text{V}.$$

In order to measure  $i$  and  $v$ , Tektronix probes A622 for current and P5200A for voltage, respectively, were used.

Regarding the inverter, four transistors IRF640 and two ICs IR2113 were chosen. On the other hand, the DC motor used was the GNM5440E-G3.1 (24 V, 95 W), whose parameters are:

$$\begin{aligned} R_a &= 0.965 \, \Omega, & k_m &= 120.1 \times 10^{-3} \frac{\text{N}\cdot\text{m}}{\text{A}}, \\ L_a &= 2.22 \, \text{mH}, & k_e &= 120.1 \times 10^{-3} \frac{\text{V}\cdot\text{s}}{\text{rad}}, \\ J &= 118.2 \times 10^{-3} \, \text{kg}\cdot\text{m}^2, & b &= 129.6 \times 10^{-3} \frac{\text{N}\cdot\text{m}\cdot\text{s}}{\text{rad}}. \end{aligned}$$

Signals  $i_a$  and  $\omega$  were measured via an A622 current probe and an encoder E6B2-CWZ6C, respectively.

*ETEDPOF control*. The control based on ETEDPOF (15) is programmed here. Gains  $\gamma_1$  and  $\gamma_2$  were selected as:

$$\gamma_1 = 0.0004, \quad \gamma_2 = 0.0002.$$

Meanwhile, the reference variables  $i^*$ ,  $i_a^*$ ,  $u_{1av}^*$ , and  $u_{2av}^*$  are generated as a result of introducing the reference trajectories  $v^*$  and  $\omega^*$  in (16)–(19).

**Board and conditioning circuit.** In this block, the connections of the DS1104 board and the conditioning circuit with the system and the control block are shown. The DS1104 board generates PWM signals that allow proper driving of converter and inverter. Whereas, the conditioning circuit electrically isolates the DS1104 board from the system via optoisolators of the models NTE3087 and TLP250.

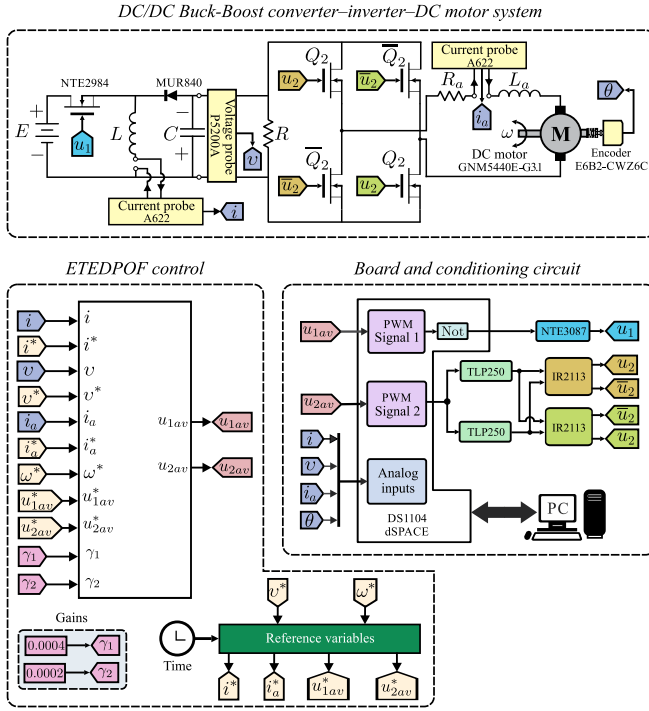


Figure 2. Electronic diagram and connections of the system in closed-loop.

A picture of the built experimental prototype, associated with the diagram in Fig. 2, is presented in Fig. 3.

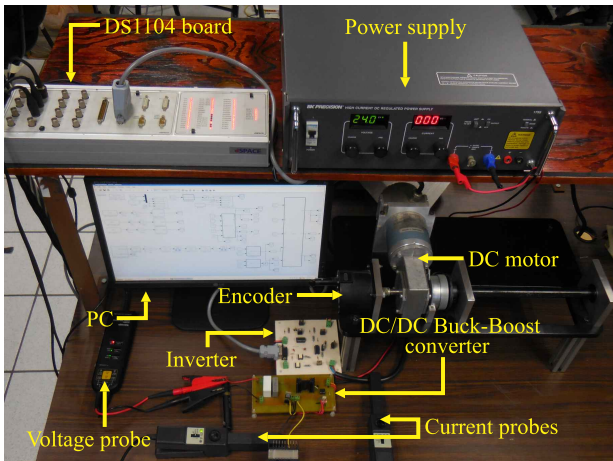


Figure 3. Picture of the built experimental prototype.

## B. Experimental results

In order to show the effectiveness of the proposed control, the experimental results obtained in closed-loop are presented here.

With the aim of supplying suitable voltage levels to the DC motor, in all the experiments the desired voltage  $v^*$  is given by the following Bézier polynomial:

$$v^*(t) = \bar{v}_i(t_i) + [\bar{v}_f(t_f) - \bar{v}_i(t_i)] \varphi(t, t_i, t_f), \quad (20)$$

where

$$\varphi(t, t_i, t_f) = \begin{cases} 0 & \text{for } t \leq t_i, \\ \left( \frac{t-t_i}{t_f-t_i} \right)^3 \left[ r_1 - r_2 \left( \frac{t-t_i}{t_f-t_i} \right) \right] \\ + r_3 \left( \frac{t-t_i}{t_f-t_i} \right)^2 - r_4 \left( \frac{t-t_i}{t_f-t_i} \right)^3 & \text{for } t \in (t_i, t_f), \\ 1 & \text{for } t \geq t_f, \end{cases}$$

with

$$r_1 = 20, \quad r_2 = 45, \quad r_3 = 36, \quad r_4 = 10,$$

and

$$\bar{v}_i = -25 \text{ V}, \quad \bar{v}_f = -30 \text{ V}.$$

It is worth mentioning that  $\bar{v}_i$  and  $\bar{v}_f$  are proposed considering (19) under steady-state, where the interaction of  $\bar{v}$ ,  $\bar{\omega}$ , and  $\bar{u}_{2av}$  is observed. The reference trajectory  $v^*$  smoothly interpolates between the initial and final voltages  $\bar{v}_i$  and  $\bar{v}_f$ , respectively, in the time interval  $[t_i, t_f]$ . Here,  $t_i = 4$  s and  $t_f = 6$  s. With the intention of verifying the performance of the system in closed-loop, the desired angular velocity  $\omega^*$  is defined in each experiment as a bidirectional trajectory.

**Experiment 1.** Here,  $v^*$  is defined as in (20) and  $\omega^*$  is proposed as follows:

$$\omega^*(t) = \bar{\omega}_i(t_i) + [\bar{\omega}_f(t_f) - \bar{\omega}_i(t_i)] \varphi(t, t_i, t_f), \quad (21)$$

with  $\bar{\omega}_i = -10 \frac{\text{rad}}{\text{s}}$  and  $\bar{\omega}_f = 10 \frac{\text{rad}}{\text{s}}$ . Values for  $[t_i, t_f]$  and  $\varphi$  were previously defined.

The experimental results in closed-loop, when  $v^*$  and  $\omega^*$  are proposed as in (20) and (21), are presented in Fig. 4. In this figure, it can be observed that the ETEDPOF control solves the tracking task for  $v$  and  $\omega$ . However, for  $i$  and  $i_a$ , there is significant tracking error. This, is due to the idealization of the mathematical model.

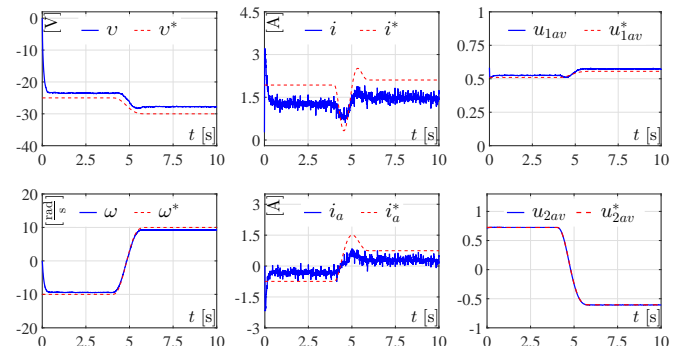


Figure 4. Results of the experiment 1.

*Experiment 2.* In this experiment  $v^*$  is proposed again as in (20) and  $\omega^*$  is chosen as:

$$\omega^*(t) = 10 \sin(0.8\pi t). \quad (22)$$

The corresponding experimental results are presented in Fig. 5. In such results, a satisfactory performance of the proposed control is presented, where a small tracking error for  $v$  and  $\omega$  is observed. Regarding  $i$  and  $i_a$ , it is observed that there is a larger tracking error. This is due to energy losses were not considered in the mathematical model.

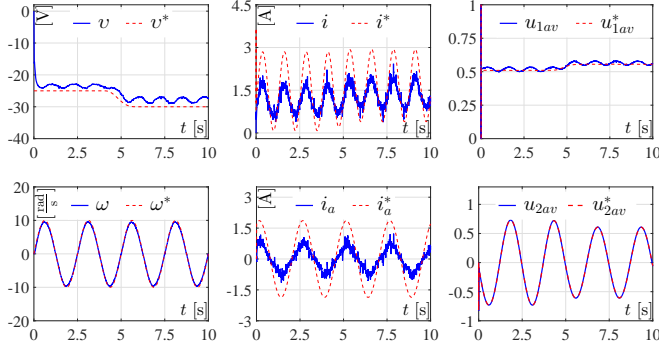


Figure 5. Results of the experiment 2.

*Experiment 3.* In this experiment, the voltage  $v^*$  is defined by (20) and the angular reference velocity by,

$$\omega^*(t) = 10 \left(1 - e^{-0.2t^2}\right) \sin(2t). \quad (23)$$

The experimental results in closed-loop are depicted in Fig. 6, where, in general, a satisfactory trajectory tracking for  $v$  and  $\omega$  is observed. Meanwhile,  $i$  and  $i_a$  versus  $i^*$  and  $i_a^*$ , differ in magnitude but not in form.

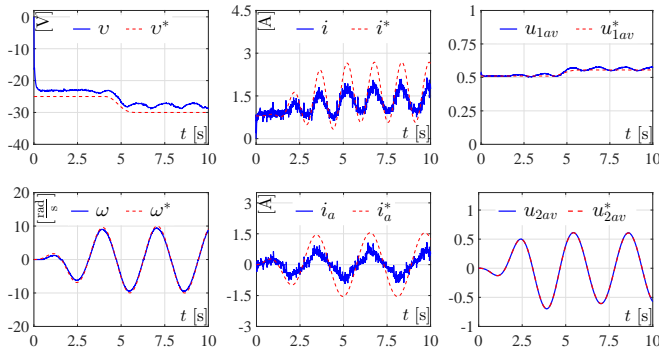


Figure 6. Results of the experiment 3.

*Experiment 4.* In Fig. 7 the dynamic behavior of the system in closed-loop is presented when  $v^*$  corresponds to (20) and  $\omega^*$  to

$$\omega^*(t) = \begin{cases} 10 & 0 \leq t < 3.125 \text{ s,} \\ 10 \sin(0.8\pi t) & 3.125 \leq t \leq 10 \text{ s.} \end{cases} \quad (24)$$

*Experiment 5.* With the aim of evaluating the system performance when abrupt variations are considered, the following change in  $R$  is proposed:

$$R_m = \begin{cases} R & 0 \leq t < 7.5 \text{ s,} \\ 30\%R & 7.5 \leq t \leq 10 \text{ s.} \end{cases} \quad (25)$$

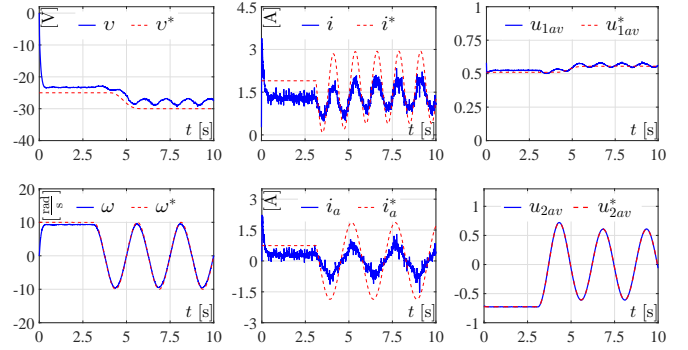


Figure 7. Results of the experiment 4.

Trajectories  $v^*$  and  $\omega^*$  considered in *Experiment 5* are defined in (20) and (21). The associated experimental results are presented in Fig. 8. Since the control based on ETEDPOF is not robust, a tracking error for  $v$  and  $\omega$  will remain from  $t \geq 7.5$  to the end of the experiment.

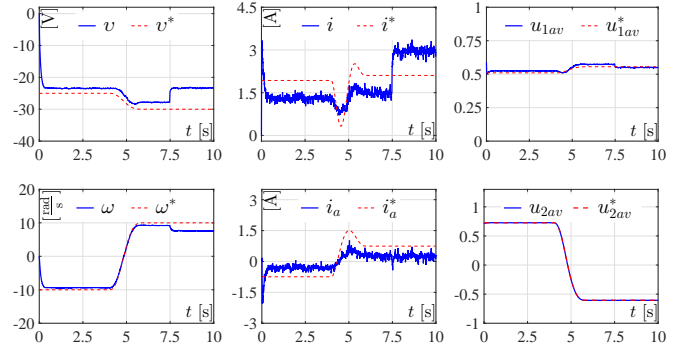


Figure 8. Results of the experiment 5.

### C. General comments on experimental results

In the experimental results in closed-loop presented in Figs. 4–7, it was observed, in general, a good trajectory tracking for  $v$  and  $\omega$ . On the other hand, the shape of  $i$  and  $i_a$  are similar to  $i^*$  and  $i_a^*$ , respectively, but in magnitude a tracking error can be observed. However, such a tracking error could be minimized if a more complete mathematical model, associated with the Buck-Boost converter, considering parasitic resistances and energy losses were used. By doing so, the designed control would be more complex and out of the objective of the paper. Regarding the inputs  $u_{1av}$  and  $u_{2av}$ , it is observed that they are not saturated; which allows the appropriate driving of the Buck-Boost converter and inverter. Also, it is worth mentioning that oscillations in Figs. 5–7 are due to the selection of the desired trajectories for  $\omega$ .

## VI. CONCLUSIONS

A passivity-based tracking control, whose experimental implementation only requires electrical measurements, for the DC/DC Buck-Boost converter–inverter–DC motor system was herein presented. This control system allows the driving of bidirectional angular velocities.

The proposed control based on the ETEDPOF was experimentally implemented using Matlab-Simulink and the DS1104 board in a built prototype, achieving satisfactory results in voltage and angular velocity tracking.

Motivated by the experimental results, particularly those in Fig. 8, the design of robust controls as well as an application in mobile robotics (see [2], [3], and [33]) are considered as future work.

## REFERENCIAS

- [1] K. Erenturk, "Hybrid control of a mechatronic system: Fuzzy logic and grey system modeling approach," *IEEE/ASME Trans. Mechatron.*, vol. 12, no. 6, pp. 703–710, Dec. 2007.
- [2] R. S. Ortigoza, J. R. G. Sánchez, V. M. H. Guzmán, C. M. Sánchez, and M. M. Aranda, "Trajectory tracking control for a differential drive wheeled mobile robot considering the dynamics related to the actuators and power stage," *IEEE Latin Am. Trans.*, vol. 14, no. 2, pp. 657–664, Feb. 2016. [Online]. Available: <http://www.ehw.ieee.org/reg/9/etras/esp/publicaciones.php>
- [3] J. R. G. Sánchez, S. T. Mosqueda, R. S. Ortigoza, M. A. Cruz, G. S. Ortigoza, and J. de J. Rubio, "Assessment of an average tracking controller that considers all the subsystems involved in a WMR: Implementation via PWM or Sigma-Delta modulation," *IEEE Latin Am. Trans.*, vol. 14, no. 3, pp. 1093–1102, Mar. 2016. [Online]. Available: <http://www.ehw.ieee.org/reg/9/etras/esp/publicaciones.php>
- [4] E. Fernández, L. Romeral, and V. Salas, "Power converters and its application in electric traction systems. Analysis present and future technologies," *IEEE Latin Am. Trans.*, vol. 14, no. 2, pp. 631–638, Feb. 2016.
- [5] F. Gao, S. Bozhko, A. Costabeber, G. Asher, and P. Wheeler, "Control design and voltage stability analysis of a droop-controlled electric power system for more electric aircraft," *IEEE Trans. Ind. Electron.*, vol. 64, no. 12, pp. 9271–9281, Dec. 2017.
- [6] M. A. Ahmad, R. M. T. Raja Ismail, and M. S. Ramli, "Control strategy of Buck converter driven DC motor: A comparative assessment," *Australian J. Basic Appl. Sci.*, vol. 4, no. 10, pp. 4893–4903, Oct. 2010.
- [7] O. Bingöl and S. Paçacı, "A virtual laboratory for neural network controlled DC motors based on a DC-DC Buck converter," *Int. J. Eng. Educ.*, vol. 28, no. 3, pp. 713–723, Jan. 2012.
- [8] H. Sira-Ramírez and M. A. Oliver-Salazar, "On the robust control of Buck-converter DC-motor combinations," *IEEE Trans. Power Electron.*, vol. 28, no. 8, pp. 3912–3922, Aug. 2013.
- [9] R. Silva-Ortigoza, J. R. García-Sánchez, J. M. Alba-Martínez, V. M. Hernández-Guzmán, M. Marcelino-Aranda, H. Taud, and R. Bautista-Quintero, "Two-stage control design of a Buck converter/DC motor system without velocity measurements via a  $\Sigma - \Delta$ -modulator," *Math. Probl. Eng.*, vol. 2013, pp. 1–11, Apr. 2013. [Online]. Available: <https://www.hindawi.com/journals/mpe/2013/929316>
- [10] R. Silva-Ortigoza, C. Márquez-Sánchez, F. Carrizosa-Corral, M. Antonio-Cruz, J. M. Alba-Martínez, and G. Saldaña-González, "Hierarchical velocity control based on differential flatness for a DC/DC Buck converter-DC motor system," *Math. Probl. Eng.*, vol. 2014, pp. 1–12, Apr. 2014. [Online]. Available: <https://www.hindawi.com/journals/mpe/2014/912815>
- [11] S. G. Kumar and S. H. Thilagar, "Sensorless load torque estimation and passivity based control of Buck converter fed DC motor," *Sci. World J.*, vol. 2015, pp. 1–15, Feb. 2015.
- [12] R. Silva-Ortigoza, V. M. Hernández-Guzmán, M. Antonio-Cruz, and D. Muñoz-Carrillo, "DC/DC Buck power converter as a smooth starter for a DC motor based on a hierarchical control," *IEEE Trans. Power Electron.*, vol. 30, no. 2, pp. 1076–1084, Feb. 2015. [Online]. Available: <http://ieeexplore.ieee.org/xpl/articleDetails.jsp?arnumber=6767144>
- [13] V. M. Hernández-Guzmán, R. Silva-Ortigoza, and D. Muñoz-Carrillo, "Velocity control of a brushed DC-motor driven by a DC to DC Buck power converter," *Int. J. Innov. Computing Inform. Control.*, vol. 11, no. 2, pp. 509–521, Apr. 2015. [Online]. Available: <http://www.ijicic.org/ijicic-14-04031.pdf>
- [14] S. Khubalkar, A. Chopade, A. Junghare, M. Aware, and S. Das, "Design and realization of stand-alone digital fractional order PID controller for Buck converter fed DC motor," *Circuits Syst. Signal Process.*, vol. 35, no. 6, pp. 2189–2211, Jan. 2016.
- [15] G. Rigatos, P. Siano, P. Wira, and M. Sayed-Mouchaweh, "Control of DC-DC converter and DC motor dynamics using differential flatness theory," *Intell. Ind. Syst.*, vol. 2, no. 4, pp. 371–380, Dec. 2016.
- [16] T. K. Nizami, A. Chakravarty, and C. Mahanta, "Design and implementation of a neuro-adaptive backstepping controller for Buck converter fed PMDC-motor," *Control Eng. Pract.*, vol. 58, pp. 78–87, Jan. 2017.
- [17] J. Linares-Flores, J. Reger, and H. Sira-Ramírez, "Load torque estimation and passivity-based control of a Boost-converter/DC-motor combination," *IEEE Trans. Control Syst. Technol.*, vol. 18, no. 6, pp. 1398–1405, Feb. 2010.
- [18] A. T. Alexandridis and G. C. Konstantopoulos, "Modified PI speed controllers for series-excited DC motors fed by DC/DC Boost converters," *Control Eng. Practice*, vol. 23, pp. 14–21, Feb. 2014.
- [19] G. C. Konstantopoulos and A. T. Alexandridis, "Enhanced control design of simple DC-DC Boost converter-driven DC motors: Analysis and implementation," *Electr. Pow. Compo. Sys.*, vol. 43, no. 17, pp. 1946–1957, Oct. 2015.
- [20] Y. Sönmez, M. Dursun, U. Güvenç, and C. Yilmaz, "Start up current control of Buck-Boost converter-fed serial DC motor," *Pamukkale Univ. J. Eng. Sci.*, vol. 15, no. 2, pp. 278–283, May 2009.
- [21] J. Linares-Flores, J. L. Barahona-Avalos, H. Sira-Ramírez, and M. A. Contreras-Ordaz, "Robust passivity-based control of a Buck-Boost-converter/DC-motor system: An active disturbance rejection approach," *IEEE Trans. Ind. Appl.*, vol. 48, no. 6, pp. 2362–2371, Nov./Dec. 2012.
- [22] E. E. Jiménez-Toribio, A. A. Labour-Castro, F. Muñoz-Rodríguez, H. R. Pérez-Hernández, and E. I. Ortiz-Rivera, "Sensorless control of Sepic and Cuk converters for DC motors using solar panels," in *Proc. IEEE Int. Electr. Mach. Drives Conf.*, Miami, FL, USA, May 3–6, 2009, pp. 1503–1510.
- [23] R. S. Ortigoza, J. N. A. Juárez, J. R. G. Sánchez, M. A. Cruz, V. M. H. Guzmán, and H. Taud, "Modeling and experimental validation of a bidirectional DC/DC Buck power electronic converter-DC motor system," *IEEE Latin Am. Trans.*, vol. 15, no. 6, pp. 1043–1051, Jun. 2017. [Online]. Available: <http://www.ehw.ieee.org/reg/9/etras/esp/publicaciones.php>
- [24] R. S. Ortigoza, J. N. A. Juárez, J. R. G. Sánchez, V. M. H. Guzmán, C. Y. S. Cervantes, and H. Taud, "A sensorless passivity-based control for the DC/DC Buck converter-inverter-DC motor system," *IEEE Latin Am. Trans.*, vol. 14, no. 10, pp. 4227–4234, Dec. 2016. [Online]. Available: <http://www.ehw.ieee.org/reg/9/etras/esp/publicaciones.php>
- [25] V. H. García-Rodríguez, R. Silva-Ortigoza, E. Hernández-Márquez, J. R. García-Sánchez, M. Ponce-Silva, and G. Saldaña-González, "A DC motor driven by a DC/DC Boost converter-inverter: Modeling and simulation," in *Proc. Int. Conf. Mechatron. Electron. Automot. Eng.*, Cuernavaca, Morelos, Mexico, Nov. 22–25, 2016, pp. 78–83.
- [26] E. Hernández-Márquez, R. Silva-Ortigoza, S.-H. Dong, V. H. García-Rodríguez, G. Saldaña-González, and M. Marcelino-Aranda, "A new DC/DC Buck-Boost converter-DC motor system: Modeling and simulation," in *Proc. Int. Conf. Mechatron. Electron. Automot. Eng.*, Cuernavaca, Morelos, Mexico, Nov. 22–25, 2016, pp. 101–106.
- [27] E. H. Márquez, R. S. Ortigoza, J. R. G. Sánchez, V. H. G. Rodríguez, and J. N. A. Juárez, "A new "DC/DC Buck-Boost converter-DC motor" system: Modeling and experimental validation," *IEEE Latin Am. Trans.*, vol. 15, no. 11, pp. 2043–2049, Nov. 2017. [Online]. Available: <http://www.ehw.ieee.org/reg/9/etras/esp/publicaciones.php>
- [28] E. Hernández-Márquez, R. Silva-Ortigoza, C. A. Avila-Rea, J. R. García-Sánchez, M. Antonio-Cruz, H. Taud, S. Dong, and M. Marcelino-Aranda, "Regulation of the DC/DC Buck-Boost converter-inverter-DC motor system: Sensorless passivity based control," in *Proc. Int. Conf. Mechatron. Electron. Automot. Eng.*, Cuernavaca, Morelos, Mexico, Nov. 21–24, 2017, pp. 88–92.
- [29] J. Linares-Flores, H. Sira-Ramírez, E. F. Cuevas-López, and M. A. Contreras-Ordaz, "Sensorless passivity based control of a DC motor via a solar powered Sepic converter-full bridge combination," *J. Power Electron.*, vol. 11, no. 5, pp. 743–750, Sep. 2011.
- [30] D. R. Merkin, *Introduction to the Theory of Stability*. New York, NY, USA: Springer-Verlag, 1997.
- [31] H. Sira-Ramírez and R. Silva-Ortigoza, *Control Design Techniques in Power Electronics Devices*. London, U.K.: Springer-Verlag, 2006.
- [32] V. M. Hernández-Guzmán, V. Santibáñez, and G. Herrera, "Control of rigid robots equipped with brushed DC-motors as actuators," *Int. J. Control Autom. Syst.*, vol. 5, no. 6, pp. 718–724, Dec. 2007.
- [33] J. R. García-Sánchez, R. Silva-Ortigoza, S. Tavera-Mosqueda, C. Márquez-Sánchez, V. M. Hernández-Guzmán, M. Antonio-Cruz, G. Silva-Ortigoza, and H. Taud, "Tracking control for mobile robots considering the dynamics of all their subsystems: Experimental implementation," *Complexity*, vol. 2017, pp. 1–18, Dec. 2017. [Online]. Available: <https://doi.org/10.1155/2017/5318504>